JABG Journal of Animal Breeding & Genomics

Journal of Animal Breeding and Genomics, 2026 March, 10(1)25-32
https://doi.org/10.12972/jabng.2026.10.1.3

Print ISSN 1226-5543
Online ISSN 2586-4297

Research Article

Network propagation prioritization of GWAS candidate genes for Hanwoo carcass traits

Jae Don Oh[1,2], **Hong Sik Kong**[1,2,*]

[1]Department of Applied Biotechnology, Hankyong National University, Anseong 17579, Korea

[2]Gyeonggi Regional Research Center, Hankyong National University, Anseong 17579, Korea

*Correspondence author: kebinkhs@hknu.ac.kr

ABSTRACT

Carcass weight (CW), ribeye area (EMA), backfat thickness (BF), and marbling score (MS) are economically important carcass traits of Hanwoo cattle. However, significant signals detected by genome-wide association studies (GWASs) are often difficult to interpret mechanistically owing to their polygenic architecture and linkage disequilibrium (LD), which may obscure the causal genes and pathways. In this study, we defined candidate genes significantly reported in three Hanwoo carcass-trait GWASs as seeds and applied network propagation to Cytoscape–STRING protein–protein interaction (PPI) networks to (i) re-rank trait-specific candidates in a network-informed manner and (ii) propose additional connected candidates that were not directly observed in GWAS (non-seed connectors). After constructing a *Bos taurus* STRING network, we built trait-specific networks by including a maximum of 20 additional interactors (interactors = 20) and computed the diffusion (heat) scores and ranks. CW and EMA repeatedly prioritized growth- and skeletal/muscle development–related candidates (the PLAG1–CHCHD7 axis) among the top-ranked non-seed genes. For BF, autophagy- and insulin resistance–related candidates (BECN1 and ENPP1) were prioritized, whereas for MS, a triglyceride synthesis and lipid droplet formation candidate (GPAT4) emerged as a top-ranked non-seed gene. Overall, this approach integrates heterogeneous GWAS findings at the network level, structures trait-relevant biological pathways, and efficiently narrows down the targets for downstream validation.

Keywords: Hanwoo, carcass traits, Genome-wide association studies, Cytoscape, STRING, network propagation

INTRODUCTION

With advances in genomic technologies and the expanding adoption of genomic selection (GS), livestock breeding has shifted from pedigree-based evaluations to models that integrate high-density SNP information. In Korea, GS is increasingly being implemented to improve genomic prediction accuracy and accelerate genetic gain, supported by the establishment of large reference populations.

Genome-wide association studies (GWASs) in Hanwoo have identified genome-wide trait-associated variants and proposed major quantitative trait loci (QTL) and candidate genes for diverse carcass traits, including marbling (marbling score; MS), backfat thickness (BF), and rib-eye area (EMA), as well as the well-known carcass weight (CW)-associated region on bovine chromosome 14 (BTA14). Accumulated GWAS signals have broadened biological insights into fat metabolism and muscle development, improved the interpretability of genetic evaluations, and supported the development of genome-enabled technologies (Uffelmann et al., 2021; Kim et al., 2022; Kim & Oh., 2023).

Nevertheless, GWAS has inherent limitations. First, much of the genetic variance is explained by numerous small-effect variants ("missing heritability"). Second, association signals do not necessarily pinpoint causal variants/genes. Finally, results can be affected by population structure,

Received March 12, 2026 **Revised** March 24, 2026 **Accepted** March 24, 2026

Copyright © 2026 Korean Society of Animal Breeding and Genetics.

This is an Open Access article distributed under the terms of the Creative Commons Attribution Non-Commercial License (http://creativecommons.org/licenses/by-nc/4.0/) which permits unrestricted non-commercial use, distribution, and reproduction in any medium, provided the original work is properly cited.

environmental confounding, linkage disequilibrium (LD)-driven broad candidate regions, sample-size constraints, and genotyping array coverage. All of these contribute to reproducibility challenges (Hirschhorn and Daly, 2005; Tam et al., 2019).

To address these issues, network-based interpretation has gained attention, moving beyond single-variant or single-gene perspectives to integrate protein–protein interactions (PPI) and functional networks. Recent comparative and integrative GWASs in livestock (including Hanwoo) have shown that the reconstruction of GWAS candidates within PPI networks often reveals concentrated biological pathways—such as lipid metabolism and muscle development—around highly connected hub nodes. This suggests that network-based approaches can connect fragmented GWAS signals to coherent functional pathways and help uncover shared mechanisms among candidates reported across different studies (Cowen et al., 2017; Szklarczyk et al., 2023; Kim et al., 2024).

Accordingly, we set candidate genes significantly associated with carcass traits (CW, EMA, BF, MS) across three independent GWASs as seeds and performed network propagation in Cytoscape to (i) integrate prior GWAS evidence in a functional network context, (ii) re-prioritize candidates by incorporating neighborhood interaction information, and (iii) identify trait-specific central genes and shared/distinct modules. This strategy aims to highlight key candidates that may be missed by single-study/single-trait analyses and provide more compelling mechanistic interpretations for Hanwoo carcass traits.

MATERIALS AND METHODS

1. Study design and analytical overview

We performed PPI network–based network propagation analyses for Hanwoo carcass traits (CW, EMA, BF, and MS) using candidate genes reported in previous GWASs as seeds. This design was intended to overcome the limitations of SNP- or single-gene-centered interpretations by incorporating functional relatedness among genes and enabling network-informed prioritization and mechanistic inference. Network propagation is widely used to diffuse association evidence across networks and re-rank functionally related candidates (Cowen et al., 2017).

Table 1. List of significant candidate genes for Hanwoo carcass traits reported in three GWAS studies.

Traits	Alam et al., 2023	Kim et al., 2024	Park et al., 2026
CW	SLIT2, PACRGL, KCNIP4, RP1, XKR4, LYN, RPS20, MOS, FAM110B, UBXN2B, CYP7A1, SDCBP, NSMAF, TOX, CA8, LAP3, FAM184B, NCAPG	NSMAF, SDCBP, TOX, ACLY, SNTG1	COBL, FAM13A, HERC3, GPRIN3, SLIT2, COL22A1, FAM135B, KHDRBS3, ZFAT, ST3GAL1, NDRG1, RGS20, XKR4, PRKDC, FAM110B, UBXN2B, CYP7A1, SDCBP, NSMAF, TOX, LAP3, MED28, FAM184B, NCAPG, DCAF16, LCORL
EMA	IBSP, LAP3, FAM184B, LCORL, NCAPG, SLC30A9, BEND4		FAM184B, NCAPG, DCAF16, LCORL, SLIT2, ZNF827, C4orf51, MMAA, SMAD1, OTUD4, ANAPC10, HHIP, RBMS3, TGFBR2, CYTH3, ZDHHC4, RNF216, ACTB, FBXL18
BF	CYP7B1, ARMC1, PDE7A, CRH	PIK3CG, ANTXR2, CFH	ATG7, VGLL4, DNAJC12, SIRT1, HERC4, MYPN, TET1, CCAR1
MS	CTSZ, GNAS, VAPB, RAB22A	AATF, ACACA, MANF, NPR3, ZFR, ACTL8, ARHGEF10L	LRRFIP1, ERFE, ILKAP, TWIST2, TBC1D22A, BMP4, CGRRF1, SAMD4A, MDFIC2, MITF

CW, carcass weight; EMA, eye muscle area; BF, backfat thickness; and MS, marbling score.

2. Construction of seed candidate genes

Trait-specific seed genes were compiled from three GWASs on Hanwoo carcass traits (Alam et al., 2023; Kim et al., 2024; Park et al., 2026). To clarify the seed-selection procedure, we explicitly followed the significance or window-selection framework used in each source study. For Alam et al. (2023), candidate genes were collected from genes reported in significant SNP/QTL regions identified under the study's GWAS threshold ($p = 1 \times 10-4$). For Kim et al. (2024), candidate genes were collected from genes reported within ±200 kb of SNPs meeting the adjusted Bonferroni threshold (Group A: $p = 2.90 \times 10-5$; Group B: $p = 2.96 \times 10-5$), whereas the stricter Bonferroni threshold (Group A: $p = 1.45 \times 10-6$; Group B: $p = 1.48 \times 10-6$) was used in the source study to confirm top SNP markers. For Park et al. (2026), candidate genes were collected from genes located within 1.0 Mb genomic windows explaining >1.0% of the total genetic variance in the WssGWAS analysis. We did not re-calculate statistical significance from raw data; instead, we used the candidate genes explicitly reported in the original studies under their respective significance or window-based criteria.

3. STRING-based PPI network construction

Trait-specific PPI networks were constructed using Cytoscape (version 3.10.1; Cytoscape Consortium, San Diego, CA, USA) (Shannon et al., 2003), an open-source platform for biological network visualization and analysis. StringApp (version 2.0.1) was used to query and import interactions from the STRING database (version 12.0) (Doncheva et al., 2019; Szklarczyk et al., 2023). The species was set to *Bos taurus*, and the minimum required interaction score (combined score cutoff) was set to 0.4 (medium confidence). After we input the seed genes, network expansion was performed, with the maximum number of additional interactors set to 20. This constraint was applied to prevent excessive network growth and retain seed-centered functional modules.

4. Network propagation analysis

Network propagation was conducted on the constructed STRING networks using the Cytoscape Diffusion application (version 1.0) based on heat diffusion. Seeds were initialized with heat = 1 and non-seeds with heat = 0. Heat was then diffused across the network according to connectivity, and diffusion scores (diffusion_output_heat) were computed for each node. In this study, the diffusion score was interpreted as a relative prioritization metric within each trait-specific network rather than as a formal test statistic with a universal significance threshold. Because no permutation-based null distribution or empirical p-values were estimated, the results were interpreted primarily by descending rank and relative network proximity to the seed-defined trait module.

5. Candidate prioritization and result summarization

For each trait, the nodes were ranked in descending order of diffusion_output_heat. The results were interpreted separately for seed and non-seed genes. Seed genes with high diffusion scores were defined as core seeds (network-central candidates), whereas non-seed genes with high diffusion scores were defined as non-seed connectors (genes that were functionally connected to the seed module). Network visualization was performed in Cytoscape by mapping node color and size to diffusion scores.

RESULTS

Overview of network propagation (interactors = 20)

We defined trait-specific seed genes from the three GWASs, constructed STRING-based PPI networks, and performed network propagation using Cytoscape Diffusion. Each trait network consisted of seeds and up to 20 additional interactors (non-seeds). The total number of nodes was as follows: CW 54 (Seed 34/Non-seed 20); EMA, 42 (22/20), BF 35 (15/20), and MS 41 (21/20).

CW network (54 nodes; seed 34, non-seed 20): Top-ranked nodes by diffusion score were NDRG1 (0), COBL (1), MOS (2), RP1 (3), ST3GAL1 (4), CA8 (5), ACLY (6), RGS20 (7), LYN (8), and PRKDC (9), followed by FAM135B (10), PACRGL (11), SLIT2 (12), KHDRBS3 (13), and LAP3 (14), indicating stable retention of seed signals within the network. Among the high-scoring non-seed candidates, PLAG1 (34), CHCHD7 (35), IBSP (36), SDR16C5 (37), IMPAD1 (38), SDR16C6 (39), ZCRB1 (40), CCSER1 (41), GXYLT1 (42), and MEPE (43) were prioritized. CW therefore showed an integrated module combining a "growth/tissue architecture–cytoskeleton axis" (COBL, NDRG1, RP1) and a "metabolism/signaling regulation axis" (ACLY, LYN, RGS20), alongside growth-axis connectors (PLAG1–CHCHD7) and skeletal/extracellular matrix (ECM)-related connectors (e.g., IBSP, MEPE).

EMA network (42 nodes; seed 22, non-seed 20): Core seeds with the highest diffusion scores included CYTH3 (0), ANAPC10 (1), FBXL18 (2), ZNF827 (3), ZDHHC4 (4), RBMS3 (5), MMAA (6), HHIP (7), BEND4 (8), and SLIT2 (9). Signaling regulators TGFBR2 (13) and SMAD1 (14) were also ranked highly, together with RNF216 (11) and SLC30A9 (12). Top-ranked non-seed candidates were ABCG2 (22), MED28 (23), MEPE (24), PLAG1 (25), SMURF1 (26), FAM13A (27), KCNIP4 (28), HMGA2 (29), SMAD7 (30), and GXYLT1 (31). EMA thus highlighted the TGF-β/SMAD axis (TGFBR2–SMAD1 with SMURF1 and SMAD7 as non-seed partners), growth/body-size connectors (PLAG1, HMGA2), and a tissue architecture/ECM–skeletal linkage (MEPE), suggesting a composite module combining muscle remodeling signaling with growth-related connectivity.

BF network (35 nodes; seed 15, non-seed 20): Top-ranked core seeds were TET1 (0), CYP7B1 (1), MYPN (2), VGLL4 (3), CFH (4), ANTXR2 (5), CCAR1 (6), HERC4 (7), DNAJC12 (8), PDE7A (9), ARMC1 (10), CRH (11), ATG7 (12), SIRT1 (13), and PIK3CG (14). High-ranking non-seed candidates were FOXO3 (15), BECN1 (16), ZMYM5 (17), PIP5KL1 (18), ENPP1 (19), ENPP3 (20), LOC511161 (21), BECN2 (22), ATG14 (23), and NYAP1 (24). Therefore, BF showed a co-occurrence of epigenetic/metabolic regulation (TET1, SIRT1), lipid/sterol metabolism (CYP7B1), autophagy/cellular remodeling (ATG7), immune/microenvironment signals (CFH, ANTXR2), and PI3K signaling (PIK3CG), with diffusion-prioritizing autophagy core connectors (BECN1/BECN2/ATG14) and metabolic/signaling connectors (FOXO3, ENPP1/ENPP3).

MS network (41 nodes; seed 21, non-seed 20): The top core seeds were MDFIC2 (0), NPR3 (1), AATF (2), MANF (3), and ZFR (4), followed by ACACA (5), SAMD4A (6), ERFE (7), ARHGEF10L (8), ILKAP (9), LRRFIP1 (10), ACTL8 (11), TWIST2 (12), VAPB (13), CTSZ (14), CGRRF1 (15), MITF (16), BMP4 (17), RAB22A (18), GNAS (19), and TBC1D22A (20). The top-ranked non-seeded candidates were GPAT4 (21), CNIH1 (22), RAB3GAP1 (23), HJV (24), C13H20orf85 (25), SGSM1 (26), MC1R (27), TBC1D10A (28), RABGAP1L-2 (29), and TBC1D19 (30). MS clustered into (i) adipogenic commitment/lineage regulation (BMP4, TWIST2, MITF, and top-ranked MDFIC2), (ii) lipogenesis execution (ACACA), (iii) cell-state/stress survival (AATF and MANF), and (iv) membrane/vesicle trafficking and signaling (RAB22A, VAPB, CTSZ, and GNAS). Notably, the top non-seed connector, GPAT4, acts as a bridge between upstream differentiation/regulatory seeds and downstream triglyceride synthesis/lipid droplet formation.

Cross-trait comparison: Growth-axis connectors (PLAG1, CHCHD7) and tissue/ECM components (MEPE, GXYLT1) repeatedly appeared as high-ranking non-seed candidates for CW and EMA, reinforcing a shared "growth–tissue architecture" context. In contrast, BF was characterized by a prominent autophagy/metabolic adaptation module (BECN1/2–ATG14), whereas MS displayed a clear combination of adipogenic commitment (BMP4/TWIST2/MITF) and metabolic execution (ACACA and GPAT4), indicating trait-specific modules.

Table 2. Top-ranked seed and non-seed candidate genes (top six each) identified by network propagation analysis for each carcass trait.

Traits	Top seed genes	Top non-seed genes
CW	NDRG1, COBL, MOS, RP1, ST3GAL1, CA8.	PLAG1, CHCHD7, IBSP, SDR16C5, IMPAD1, SDR16C6.
EMA	CYTH3, ANAPC10, FBXL18, ZNF827, ZDHHC4, RBMS3.	ABCG2, MED28, MEPE, PLAG1, SMURF1, FAM13A.
BF	TET1, CYP7B1, MYPN, VGLL4, CFH, ANTXR2.	FOXO3, BECN1, ZMYM5, PIP5KL1, ENPP1, ENPP3.
MS	MDFIC2, NPR3, AATF, MANF, ZFR, ACACA.	GPAT4, CNIH1, RAB3GAP1, HJV, C13H20orf85, SGSM1.

CW, carcass weight; EMA, eye muscle area; BF, backfat thickness; and MS, marbling score.

DISCUSSION

Network propagation consistently prioritized PLAG1 and CHCHD7 as the top non-seed candidates for both CW and EMA. In the CW network, PLAG1 (heat = 0.418) and CHCHD7 (= 0.416) exhibited the highest non-seed diffusion scores, and in the EMA network, they remained among the top ranks (PLAG1 = 0.280; CHCHD7 = 0.263). These results suggest that these two traits may share genetic regulation related to growth and body size.

Additionally, the prioritization of IBSP (CW) and MEPE (EMA) among the top non-seed candidates suggests that growth signals may extend beyond simple body weight increases and may be coupled with skeletal development and ECM remodeling. This supports the interpretation of CW–EMA as an integrated module linking the body frame, muscle mass, and skeletal/ECM remodeling.

In the EMA network, the seed genes TGFBR2 and SMAD1 were highly ranked, and SMURF1 emerged as a non-seed candidate. This indicates that muscle mass formation may be closely tied not only to growth signals but also to regulation of the TGF-β/BMP–SMAD pathway. TGF-β signaling is known to play key roles in skeletal muscle regeneration, differentiation, and fibrosis control (Delaney et al., 2016). SMURF1, an E3 ubiquitin ligase involved in BMP signaling, has also been implicated in the regulation of myogenic differentiation (Ying et al., 2003). Thus, the EMA results supported a model in which growth-related genes and a muscle differentiation regulatory module act together.

For BF, the top-ranked seed TET1 and the emergence of BECN1 and ENPP1 as high-ranking non-seed candidates suggest that it may be more strongly related to metabolic homeostasis and cellular state regulation than to fat synthesis quantity alone. TET1 is an epigenetic regulator that suppresses thermogenic programs in the adipose tissues (Villivalam et al., 2020). BECN1 is an autophagy-related protein implicated in the regulation of adiponectin secretion and insulin sensitivity in the adipose tissue (Kuramoto et al., 2021). ENPP1 contributes to insulin resistance and adipocyte maturation by inhibiting insulin receptor signaling (Liang et al., 2007). Collectively, these findings support an association between BF and epigenetics–autophagy–insulin signaling axis.

For MS, the co-occurrence of the seed gene ACACA and the top-ranked non-seed candidate GPAT4 suggests that intramuscular fat deposition may be directly linked to de novo lipogenesis (DNL) downstream triglyceride synthesis and lipid droplet formation. GPAT4 is essential for triacylglycerol synthesis and lipid droplet formation (Wilfling et al., 2013), whereas ACACA is a key enzyme in fatty acid synthesis and is associated with the activation of lipogenic genes related to lipid accumulation in the muscle (da Costa et al., 2013). In addition, the highly ranked seed NPR3 (natriuretic peptide clearance receptor) has been linked to the regulation of energy expenditure in adipose tissue (Li et al., 2024), suggesting that endocrine metabolic signaling may also contribute to MS variation.

Taken together, by reinterpreting literature-derived GWAS candidates at the network level, this study delineated trait-specific functional modules, growth modules (CW and EMA), metabolic homeostasis modules (BF), and lipid synthesis modules (MS), demonstrating that GWAS candidate interpretations can be expanded from individual genes to coherent functional modules.

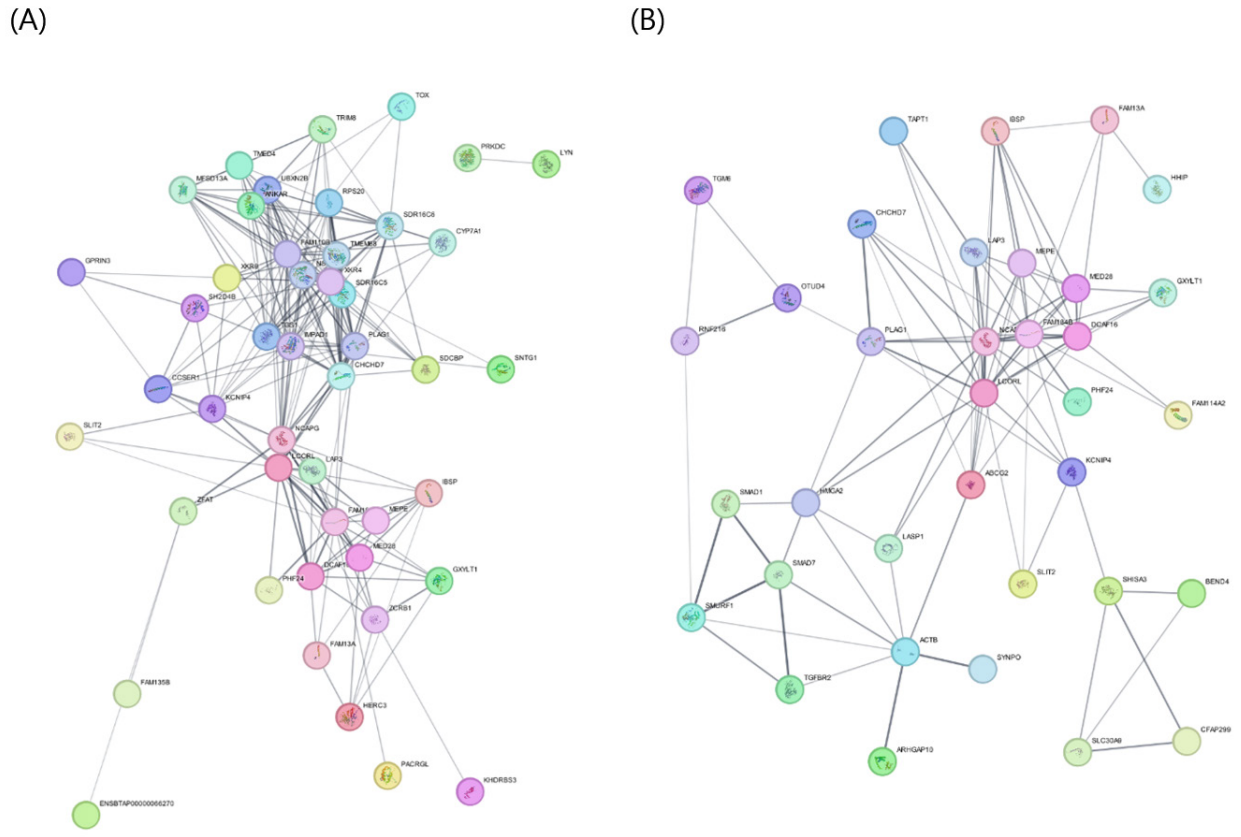

Figure 1. Protein–protein interaction networks and network propagation results for carcass traits in Hanwoo cattle. (A) Carcass weight (CW) network and (B) eye muscle area (EMA) network constructed using the STRING database and visualized in Cytoscape

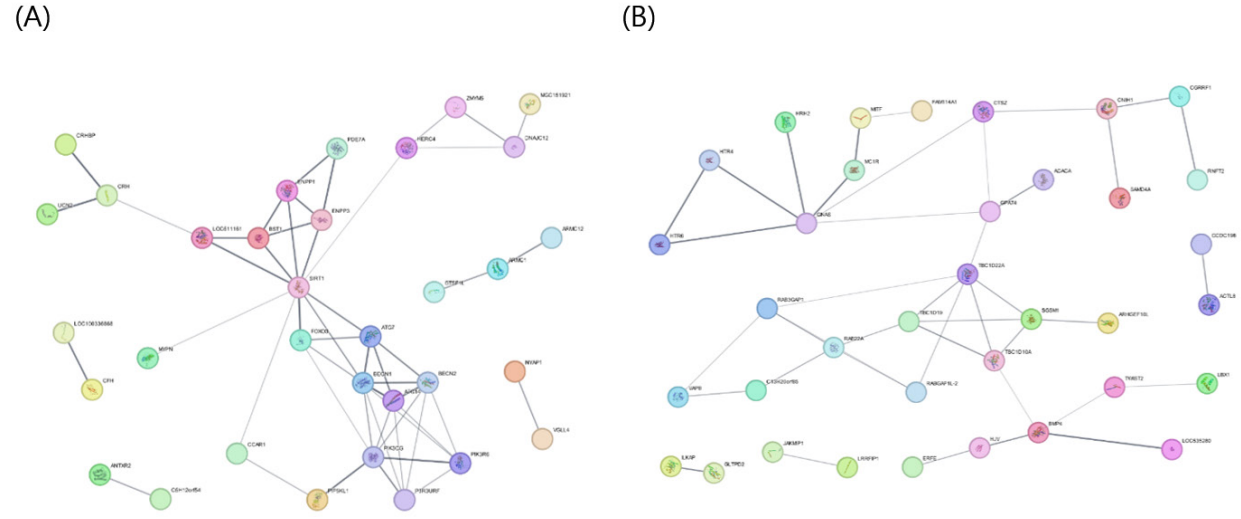

Figure 2. Protein–protein interaction networks and network propagation results for fat-related carcass traits in Hanwoo cattle. (A) Backfat thickness (BF) network and (B) marbling score (MS) network constructed using the STRING database and visualized in Cytoscape.

CONCLUSION

This study projected literature-derived candidate genes for Hanwoo carcass traits onto STRING PPI networks and applied network propagation to reinterpret the existing GWAS findings at the network level. This enabled an integrated module-based understanding of candidates reported across individual studies and identified additional non-seed connector genes that were not directly reported in the GWAS.

Trait-wise, CW and EMA shared a growth- and body-size–related module centered on the PLAG1–CHCHD7 axis, supporting genetic and functional connections between the two traits. BF highlighted genes related to autophagy and insulin signaling, centered on TET1, suggesting that fat accumulation may be closely linked to metabolic homeostasis and regulation of the cellular state. MS revealed a module centered on ACACA and GPAT4, associated with fatty acid synthesis and lipid droplet formation, supporting the core metabolic pathways underlying intramuscular fat deposition.

CONFLICT OF INTERESTS

No potential conflict of interest relevant to this article is reported.

ACKNOWLEDGEMENTS

This work was supported by a research grant from Hankyong National University in the year of 2024.

REFERENCES

Alam MZ, Haque MA, Iqbal A, Lee YM, Ha JJ, Jin S, Park B, Kim NY, Won JI, and Kim JJ. 2023. Genome-wide association study to identify QTL for carcass traits in Korean Hanwoo cattle. Animals 13:2737. https://doi.org/10.3390/ani13172737

Carlin DE, Demchak B, Pratt D, Sage E, and Ideker T. 2017. Network propagation in the Cytoscape cyberinfrastructure. PLoS Comput Biol 13:e1005598. https://doi.org/10.1371/journal.pcbi.1005598

Cowen L, Ideker T, Raphael BJ, and Sharan R. 2017. Network propagation: a universal amplifier of genetic associations. Nat Rev Genet 18:551-562. https://doi.org/10.1038/nrg.2017.38

da Costa ASH, Pires VM, Fontes CMGA, and Prates JAM. 2013. Expression of genes controlling fat deposition in two genetically diverse beef cattle breeds fed high or low silage diets. BMC Vet Res 9:118. https://doi.org/10.1186/1746-6148-9-118

Delaney K, Kasprzycka P, Ciemerych MA, and Zimowska M. 2017. The role of TGF-β1 during skeletal muscle regeneration. Cell Biol Int 41:706-715. https://doi.org/10.1002/cbin.10725

Doncheva NT, Morris JH, Gorodkin J, and Jensen LJ. 2019. Cytoscape StringApp: network analysis and visualization of proteomics data. J Proteome Res 18:623-632. https://doi.org/10.1021/acs.jproteome.8b00702

Hirschhorn JN and Daly MJ. 2005. Genome-wide association studies for common diseases and complex traits. Nat Rev Genet 6:95-108. https://doi.org/10.1038/nrg1521

Kim HJ, de Las Heras-Saldana S, Moghaddar N, Lee SH, Lim D, and van der Werf JHJ. 2022. Genome-wide association study for carcass traits in Hanwoo cattle using additional relatives' information of non-genotyped animals. Anim Genet 53:863-866. https://doi.org/10.1111/age.13251

Kim DH and Oh JD. 2023. Searching candidate genes associated with pH concentration in Hanwoo meat using GWAS and functional analysis. J Anim Breed Genom 7:65-73. https://doi.org/10.12972/jabng.20230008

Kim JY, Kim EH, Kang HC, Myung CH, Kong IK, and Lim HT. 2024. Genome-wide association study comparison analysis based on Hanwoo full-sib family. Anim Biosci 37:2054-2065. https://doi.org/10.5713/ab.24.0303

Kuramoto K, Kim YJ, Hong JH, and He C. 2021. The autophagy protein Becn1 improves insulin sensitivity by promoting adiponectin secretion via exocyst binding. Cell Rep 35:109184. https://doi.org/10.1016/j.celrep.2021.109184

Liang J, Fu M, Ciociola E, Chandalia M, and Abate N. 2007. Role of ENPP1 on adipocyte maturation. PLoS One 2:e882. https://doi.org/10.1371/journal.pone.0000882

Park J, Yu JS, Byun SK, Choe HS, and Kim DH. 2026. Weighted Single-Step Genome-Wide Association Study Identifies Candidate Genes for Carcass Traits and Primal Cut Yields in Hanwoo Cattle. Animals 16:136. https://doi.org/10.3390/ani16010136

Shannon P, Markiel A, Ozier O, Baliga NS, Wang JT, Ramage D, Amin N, Schwikowski B, and Ideker T. 2003. Cytoscape: a software environment for integrated models of biomolecular interaction networks. Genome Res 13:2498-2504. https://doi.org/10.1101/gr.1239303

Szklarczyk D et al. 2023. The STRING database in 2023: protein–protein association networks and functional enrichment analyses. Nucleic Acids Res 51:D638-D646. https://doi.org/10.1093/nar/gkac1000

Tam V, Patel N, Turcotte M, Bosse Y, Pare G, and Meyre D. 2019. Benefits and limitations of genome-wide association studies. Nat Rev Genet. https://doi.org/10.1038/s41576-019-0127-1

Uffelmann E, Huang QQ, Munung NS, et al. 2021. Genome-wide association studies. Nat Rev Methods Primers 1:59. https://doi.org/10.1038/s43586-021-00056-9

Villivalam SD et al. 2020. TET1 is a beige adipocyte-selective epigenetic suppressor of thermogenesis. Nat Commun 11:4313. https://doi.org/10.1038/s41467-020-18054-y

Wilfling F et al. 2013. Triacylglycerol synthesis enzymes mediate lipid droplet growth. Dev Cell 24:384-399. https://doi.org/10.1016/j.devcel.2013.01.013

Li SJ et al. 2024. Natriuretic peptide receptor-C perturbs mitochondrial respiration in white adipose tissue. J Lipid Res 65:100623. https://doi.org/10.1016/j.jlr.2024.100623

Ying SX, Hussain ZJ, and Zhang YE. 2003. Smurf1 facilitates myogenic differentiation and antagonizes BMP-2-induced osteoblast conversion by targeting Smad5 for degradation. J Biol Chem 278:39029-39036. https://doi.org/10.1074/jbc.M301193200